ECS Transactions, 58 (1) 209-221 (2013)
10.1149/05801.0209ecst ©The Electrochemical Society

Oscillation of PEFC under Low Cathode Humidification: Effect of Gravitation and Bipolar Plate Design

Daniel G. Sanchez[a] , Alfredo Ortiz[b], K. Andreas Friedrich[a].

[a]Deutsches Zentrum für Luft und Raumfahrt (DLR), Institut für Technische Thermodynamik, Pfaffenwaldring 38-40, 70569 Stuttgart, Germany.
[b]Dpto. Ingeniería Química y QI. ETSII y T, Universidad de Cantabria, Av. de los Castros s/n, 39005, Santander, Spain

Oscillatory fluctuations of a single proton exchange membrane fuel cell appear upon operation with a dry cathode air supply and a fully humidified anode stream. Periodic transitions between a low- and high-current operation point of the oscillating state due to the balance of drying and wetting processes in combination with water transport have been observed previously; however, several new aspects have been investigated in the present study, providing insight into the initiation processes. The oscillations are caused by periodic flow type changes from one- to two-phase flow in the anodic channels of the flow field. It has been observed that cell orientation with respect to Earth's gravity field affects the liquid water distribution in the anodic flow channels and, thus, also affects the oscillatory behavior of the cell performance.

Introduction

Polymer electrolyte membrane fuel cells (PEMFCs) are expected to play an important role in the future for energy supply when hydrogen is available as a fuel. As electrochemical energy converters, these fuel cells enable the direct and efficient conversion of hydrogen energy into power for stationary, portable and automobile applications. An efficient and reliable operation of fuel cells requires a comprehensive understanding of the underlying physicochemical processes (1-2). Water management represents one of the main challenges in the design and operation of PEMFCs. Maintaining proper membrane humidity is one of the key requirements to reach optimum performance, which is especially necessary for automotive applications (3-6). Water management is generally provided through external pre-humidification of the reactant gases and by the water generated in the cell reaction. However, in some applications, the extra size and weight of the humidifier should be avoided (7). Imbalance between production and evaporation rates can result in either flooding of the electrodes or membrane dehydration, both of which severely limit fuel cell performance and fuel cell life (8-10).

Among the mechanisms of water transport, electro-osmotic drag and back diffusion are functions of the fuel cell temperature, current density and membrane water content (humidity). Phase change processes occur until the equilibrium states are achieved. However, whether phase equilibriums of water exist remain debated because of the presence and arbitrary transport of liquid water, especially in the heterogeneous structures of the CL and GDL (11-15).

Several experimental works have described water management and the self or partial humidification operation without external humidification, demonstrating stable operation

states in some cases (16-18). Additionally, numerous studies have presented theoretical models using computational fluid dynamics (CFD) software to describe water transport in PEMFCs, through which the instability of the fuel cell system could be explained (19-21). Simulation results have shown that a cathode humidifier is necessary to maintain a high water content of the fuel cell membrane, whereas an anode humidifier is not needed. The performance of the humidifier is affected by the inlet air and water conditions, such as the flow rate, temperature and relative humidity (22-25). Experimental and theoretical studies have revealed nonlinear responses, such as multiple steady states as well as periodic oscillations. Studied oscillations in PEMFCs can result from either poisoning effects of the catalysts (26) or complex water management. The study of the current oscillations under low cathode hydration has been the focus of several research groups recently, with the aim of understanding the variables that control the phenomenon and its origin (11, 27-29).

To achieve a better understanding of the electrochemical processes in PEMFCs and to investigate the effects of operating conditions on the local performance, a variety of locally resolved current density distribution mapping techniques have been developed (6). Among these techniques, segmented fuel cell technology is one of the important technologies applied for the in-situ detection of the fuel cell system. Sánchez et al. (28) have presented current density distributions for drying changes with high and low cell currents at distinct times, indicating a propagating active area with defined boundaries with a downward transition period that strongly depends on the operation conditions.

The oscillatory behavior of the cell performance induced by large humidity gradients from the wet anode to dry cathode air is significant as it allows us to understand and evaluate some of the processes related to the management of water in PEMFCs. In particular, there are interesting features in the oscillation that have the potential for advancing the understanding of water interaction in the cell: (i) the downward transition associated with dehydration of the membrane, which has a considerable stability and can be studied using in situ techniques (e.g., electrochemical impedance spectroscopy (EIS) in segments); (ii) a transient high current operation point that corresponds to the steady state of the cell under optimum hydration conditions; and (iii) a characteristic upward transition time that does not depend on operation conditions for a membrane system.

The rate of transition between the high to low level (corresponding to a change from the hydrated to dehydrated cell) depends markedly on the drying conditions and the amplitude of the oscillations, which permits direct comparison of the dehydration degree of the cell under the operational conditions and the design selected. However, the high level indicates the full performance potential of the cell at any time and can be used for determining degradation rates. Although the controlling mechanism of transition from the low- to high-current state has not been completely clarified, it is clear that the mechanism is associated with the presence of liquid water in the anode channel. Some models have been proposed to describe this transition, as it is analyzed in the work reported by Nazarov et al. (30), which does not include local resolution, or in the recent work by Sanchez et al. (28), which proposes a simple model to describe the drying process. This study relates the amplitude of the oscillations to the amount of H_2O in the membrane. It is known that the transition from low to high currents, often called ignition in the literature, depends strongly on anode local processes, as was discussed by Atkins et al. (27) and confirmed by in situ current density distribution measurements (11).

In this paper, we present several advances in the understanding of the oscillatory fluctuations under dry cathode air supply and wet anode hydrogen flow conditions. First, a comparison between the galvanostatic and potentiostatic measurements in combination

with variations of anode humidity and cathode flows provides insight into their effects on the oscillatory amplitude and frequency. Second, a clear correlation of the transition from low to high performance with the existence of liquid water in the anode and the importance of forced water convection is demonstrated. The measured effect of the oscillatory behavior on the orientation of the PEMFC with respect to Earth's gravity field further supports this interpretation. This study provides the essential insight necessary for a future complete model description of PEFC oscillations.

Experimental set-up

The dynamic response of polymer electrolyte fuel cells was investigated on single cells with an electrode area of 25 cm^2 at in-house-developed testing stands of the German Aerospace Center (DLR). The test bench, controlled by programmable logic controllers (PLCs), allows automatic control of the input and output conditions, such as the pressure, temperature, flow rate of gases and humidity of reactants. The gas mass flow rates (air and H2) were controlled through the test station and could be varied between 0 and 500 ml min^{-1} on the anode side and between 0 and 2000 ml min^{-1} on the cathode side. The pressure was fixed at 1500 mbar for the experiment. The reference operating conditions are summarized in Table 1. Co-flow and counter-flow configurations of the flow fields were used in the present study. The relative humidity of the inlet gases was controlled through water-filled, heated sparger bottles.

These testing stands have the possibility to by-pass the bubblers and introduce dry gases into the cell. A relative humidity (RH) of approximately 5% was applied to the cathode side under dry conditions, which was accomplished by introducing ambient (20°C) gas using the bubbler by-pass.

Commercial electronic loads were used in the test stands and for the measurements. Here, the galvanostatic and potentiostatic modes were used, meaning that the cell current or voltage was kept constant, whereas the corresponding voltage or current changed with time by adjusting itself to the power generation.

TABLE I. Experimental conditions

Potentiostatic mode:	600 mV
Galvanostatic mode:	15 A
Flow Anode (H2):	209 ml/min
Flow Cathode (Air):	664 ml/min
Bubbler Anode temperature	80 °C
Cell temperatures :	80 °C
Pressure:	1.5 bar
Relativity humidity Anode (H2):	100%
Relativity humidity Cathode (Air):	ca. 5%

The active area of the cell was 25 cm^2 (5 cm x 5 cm), and the membrane electrode assembly (MEA) was a commercial Nafion®-111-IP with an anode and cathode Pt loading of 0.3 mgPt cm–2 on each side (Ion Power Inc. Company). For the GDL, a SGL Group Sigracet® 35 BC was used for all measurements.

Most in situ methods used in fuel cells are integral and, therefore, do not allow a locally resolved analysis of the cell. However, it is important to obtain local information as inhomogeneous distribution of reactants and products often occurs depending on the operating conditions. In the present experiments, locally resolved current density

measurements in a single cell were performed to gain insight into the nature of the oscillating fluctuations. The configuration for the single serpentine flow field is illustrated in Figure 1. The channel cross-section is 0.1 cm x 0.1 cm.

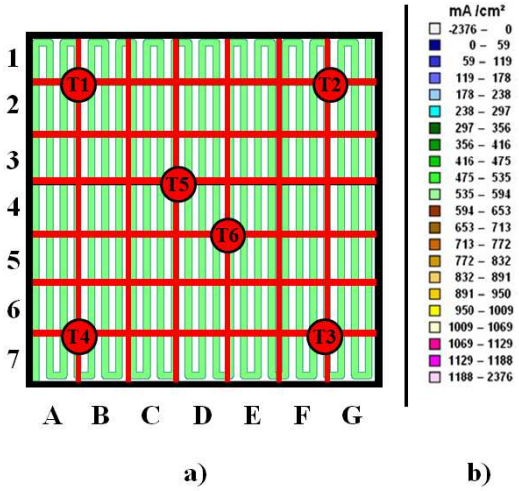

Figure 1. Single serpentine segmented cell design: (a) segment distributions with T1-T6 indicating the location of the temperature sensors and (b) color code for current density ranges**.**

A segmented bipolar plate based on printed circuit board (PCB) technology with integrated temperature sensors was used in the single cell to investigate the locally resolved current density distributions (31-32). The temperature sensors are needed for resistance calibration and to maintain an isothermal measurement; the PCB board was introduced at the anode side.

The present work also demonstrates the effect of the orientation of the bipolar plates on the oscillatory phenomena to evaluate the effect of the gravity field. Four different configurations, as illustrated in Figure 2, are used to study the effect of gravity on the cell performance.

1. Configuration 1 has the MEA perpendicular to the Earth's surface, and the channels are parallel to this surface.
2. Configuration 2 has the MEA and the channels perpendicular to the Earth's surface plane.
3. Configuration 3 has the MEA parallel to the surface plane with the cathode up and the anode down.
4. Configuration 4 has the MEA parallel to the surface plane with the cathode down and the anode up.

Most of the experiments were performed using configuration 1. Only the results presented in Figures 12 and 14 correspond to different configurations.

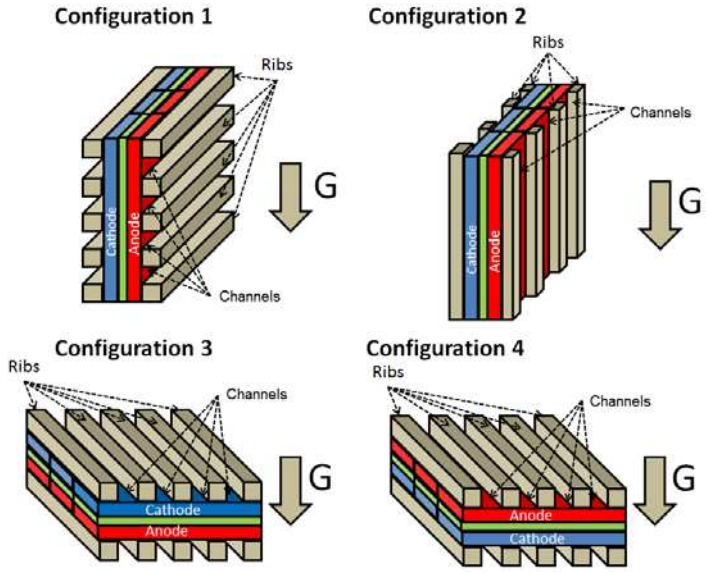

Figure 2. The four orientations used to study the effect of gravitation on cell performance.

Results and Discussion

This work is intended to complement previous studies that focused on the oscillatory response of a single proton exchange membrane fuel cell under pronounced humidity differences between the anode (wet) and cathode (dry) compartments. Insight into the transitions between high- and low-current operation points is obtained based on current density distributions at distinct times, indicating a propagating active area with defined boundaries. We aim to contribute to the understanding of the phenomena associated with water management within the fuel cell.

Even though the conditions of normal stack operation vary considerably compared with the conditions under which oscillatory fluctuations appear, several groups have been interested in this phenomena (11, 27, 29). The reason for this interest is that water transport plays a crucial role in fuel cell performance and reliable operation. However, water transport in a fuel cell depends on the flow rate dependent influx and removal, pressures, electroosmotic drag, the reaction rate and back diffusion. Therefore, the complex effect of water transport on current voltage curves cannot be currently modeled in an unambiguous way. The appearance of oscillations under humidity gradient conditions opens the path to a much better understanding of water transport properties due to the distinct effects of transient behavior on operation conditions and the possibility of experimentally validating two-phase flow models with high accuracy. A model that accurately describes the oscillatory behavior will have superior predictive potential for fuel cell operation in general.

In principle, oscillatory behavior requires two states with stability at the same operation conditions of the cell. In our case, the driving force for the oscillation is the humidity gradient from the anode to cathode, which is responsible for the two opposing processes: the drying process from the cathode side, which reduces performance, and the wetting process from the anode side, which compensates for the drying effect. We demonstrate that a minimum water quantity on the anode side is needed to overcome the drying effect. The balance between these two processes determines the minimum performance level, the amplitude and the frequency associated with the oscillatory behavior. One factor is the minimum performance level, which is determined by the

threshold amount of water provided at the anode as demonstrated by Sanchez et al. (11). Without this minimum anode humidity, the oscillatory behavior is not perceived. Other characteristic quantities are the oscillation amplitude and frequency. Oscillations have been reported for cathode relative humidities from approximately 5 – 70 % and anode humidities from approximately 75 - 135 %. The humidity gradient is as important as the pressures and gas flow rates.

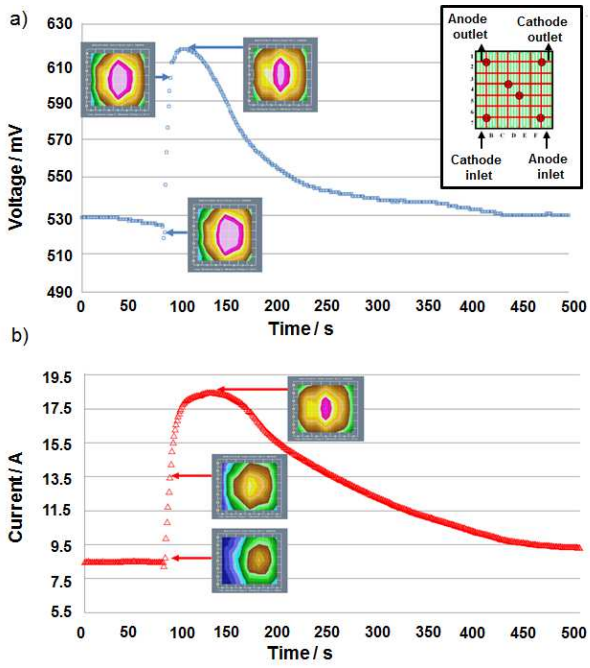

Figure 3. (a) Galvanostatic operation at 20 A and (b) potentiostatic operation at 600 mV and the corresponding current density distributions for a counter-flow configuration with the operation parameters of table 1 are presented.

The amplitude of the oscillations are highly related to the local amount of H_2O in the membrane, as reported in previous works. In Figure 3, a comparison of the oscillatory behavior for (a) galvanostatic and (b) potentiostatic operation is provided, and the corresponding current density distributions for a counter-flow configuration with the operation parameters of Table 1 are presented. Oscillations in electrochemical systems are related to the negative impedance characteristics of the faradaic processes at the electrode and are normally observed under strictly galvanostatic or potentiostatic conditions. Therefore, it is of interest that periodic transitions between a low- and high-current operation point of the oscillating state are observed for both operation modes. The transition time of 20-25 s for the change from the low to the high operation is fast and does not depend on the operating parameters, while the downward transition depends strongly on the operating conditions. The current density distributions at distinct times for high and low currents indicate that the transitions are associated with a propagating active area with defined boundaries for both operation modes under this flow configuration. The observations agree with the assumption of a liquid water reservoir at the anode with a downward transition period depending on the operation conditions. The high-current operation possesses a high electro-osmotic drag and a high permeation rate (corresponding to liquid-vapor permeation), leading to a large water flux to the cathode. Subsequently, the liquid reservoir at the anode is consumed, leading to drying of the

anode. The system establishes a new quasi-stable operation point associated with a low current, low electro-osmotic drag coefficient, and low water permeation (corresponding to vapor-vapor permeation). When liquid water is formed at the anode interface, a fast transition to the high-current operation occurs after a period of time due to the flooding effect leading to blockage of channels.

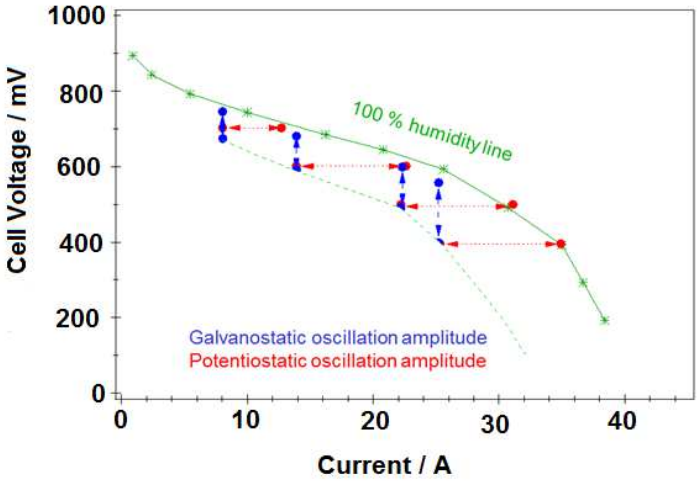

Figure 4. Comparison of the oscillation amplitudes of galvanostatic (dotted red line) and potentiostatic operation (broken blue line) with the current voltage curve at 100% RH (stoichiometric ratio: 1.5 (H_2) and 2 (Air)).

Figure 4 compares the amplitudes determined from the oscillations in galvanostatic and potentiostatic operation at identical operation conditions for 100 % RH on the anode side and approximately 5% RH on the cathode side with the current voltage curve determined from this cell at constant 100 % RH conditions. It can be observed that both operation modes exhibit the same limiting high or low performances within measurement error, which correspond to these operation conditions. It can be concluded that for both operation modes, the upper limit of performance corresponds to the full (optimum) humidification of the cell, whereas the lower operation point corresponds to an extrapolated stable current voltage curve for reduced humidity conditions. In this case, the comparison is made at constant stoichiometries of the anode (λ_{H2}=1.5) and cathode (λ_{Air}=2), which implies that the flow rates vary along the current voltage curves. Next, we will discuss measurements where the flow rate is kept constant to maintain the same water influx and removal rates.

It is interesting to investigate the effect of different RH values at the anode side to determine the importance of the driving force of the humidity gradient for the oscillations. The measurements at three different RHs at the anode are presented in Figure 5 for galvanostatic operation.

These experiments demonstrate that the “ignition” transition from low to high current levels requires a minimum value of RH on the anode side to occur. With RH values at the anode lower than 72% (triangles), ignitions were not observed. At a RH of 72 %, the humidity gradient is low, and the water amount in the cell is also reduced, which leads to small fluctuations (very small amplitude) at low performance of the cell. Increasing the RH on the anode side from 72% to 100% (squares) corresponds to an additional 22% in the net amount of water in the anode, which induces the ignition transition, leading to pronounced voltage amplitudes and characteristic times of approximately 400 s between

the low-performance regions, which are the more durable conditions of the cell. For these conditions, the high-performance operation point tends to appear as duplets, and the amplitude is approximately 100 mV between the low- and high-performance points. Increasing the anode RH from 100% to 135% (circles) involves a 40% addition to the net water amount in the anode side and results in a higher ignition frequency. Now, the characteristic time between low operation performances is only in the range of 50-80 s, and the amplitude is reduced to 50 mV. The high-performance operation seems to be more stable than the low-performance operation point. With this series, it can be concluded that the amplitude is maximized after reaching a threshold value and diminishes with increasing water content at the anode.

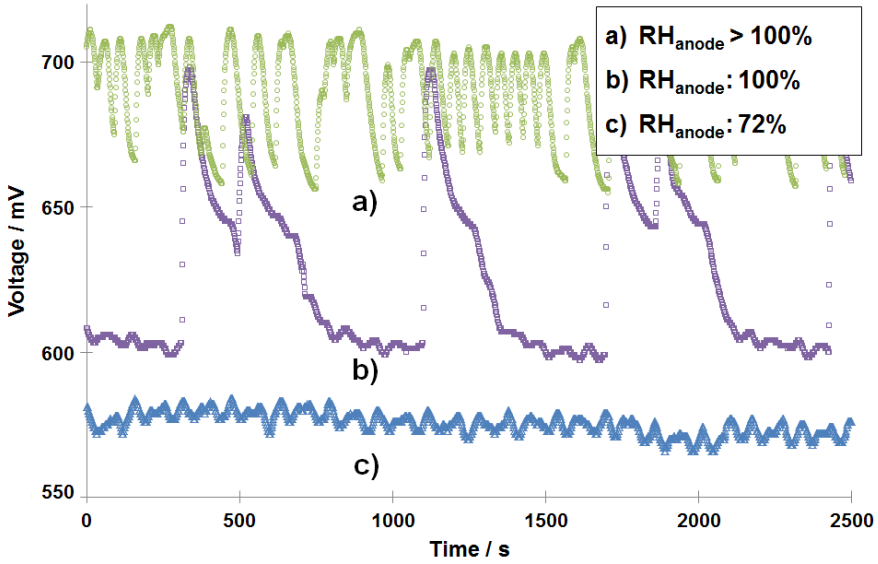

Figure 5. Effect of the anode RH on the oscillation behavior, anode RH of: 72% (triangles), 100% (circles) and 137% (diamonds); other parameter values according to table 1 conditions.

Increasing the amount of water in the anode inlet can counteract the drying process in the cell from the cathode side, which results in a more stable response with increased performance (with a decrease in the oscillating amplitude). This result is consistent with previous works (11, 29).

Pressure peaks are related to the presence of two-phase water (vapor and liquid) in the anode channel as liquid water blocks the single serpentine channel and concurrently leads to pressure inlet peaks. The pressure peak apparently is concurrent with the ignition transition.

To correlate the two-phase water presence in the anode channel to the ignition transition, it is necessary to monitor the pressures at different positions in the cell, as displayed in Figure 6, where the time evolution of the cell pressures can be observed. The synchronized pressure increase in the anode inlet (red squares) and the start of the transition toward high performance is again evident, while pressure decreases somewhat at the anode outlet (orange line).

This behavior is consistent with the already proposed blocking of liquid water in the anode channel, which leads to a pressure increase in the inlet region and may lead to a forced convection of water into the membrane.

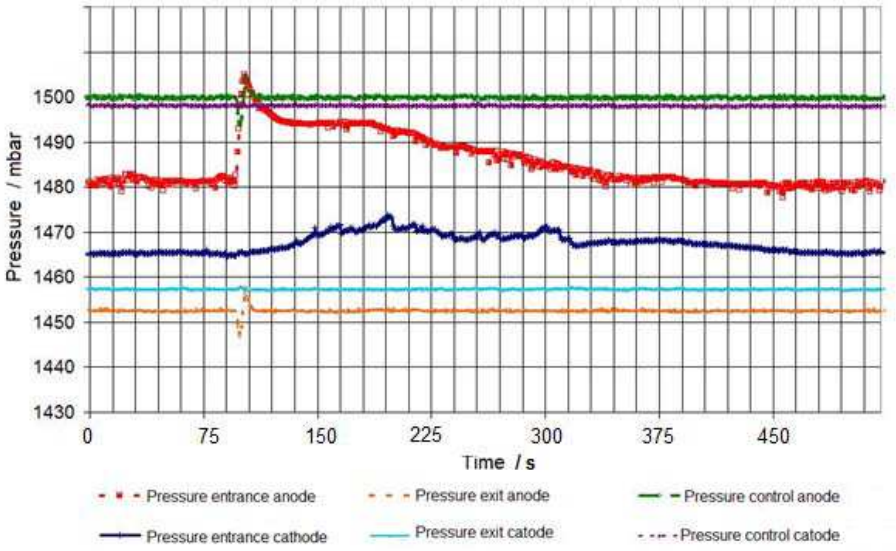

Figure 6: Pressures in the cell during the ignition event, low to high performance transition.

It may be concluded that this partial obstruction of the serpentine channel is the result of the two-phase fluid occurrence in the anode channel as demonstrated by Ly et al. 33. The liquid water can be produced spontaneously by condensation as described by Wang et al. 34. Interestingly, a pressure increase is also observed at the cathode inlet with a delay of approximately 600 - 700 ms. Liquid water also appears at the cathode channel 35 due to the ignition transition at the anode side, confirming the assumption of forced water convection through the cell.

Effect of cell orientation on transient response

Once the existence of liquid water in the anode has been related to the appearance of ignition (Figures 3-11), it seems reasonable to also expect an effect of gravity on the oscillatory phenomenology because it may contribute to the accumulation of H_2O in the liquid state in the channel 36. Therefore, different orientations of the gravity field are compared regarding their effect on the oscillations in the cell. The investigated orientations correspond to the configuration presented schematically in Figure 2.

First, configurations 1 and 2 shown in Figure 2 are compared. The analysis begins by keeping the cell in a vertical position (MEA perpendicular to the ground plane) and comparing the use of channels parallel to the ground (configuration 1) with the use of perpendicular channels (configuration 2). For both configurations, the gravity force is perpendicular to the water flow in the membrane; however, we can expect a facilitated removal of water in configuration 2, leading to a reduced channel-blocking tendency. Hence, a pronounced difference in the oscillatory behavior can be observed in Figure 7. The current density distributions for configuration 1 exhibit dramatic changes in the active surface area for the two performance levels. In contrast, in configuration 2, the differences in the current density distribution can be considered marginal. Only some smaller active spots appear for the higher performing operation points. Interestingly, the low performance current density distribution for configurations 1 and 2 are almost indistinguishable.

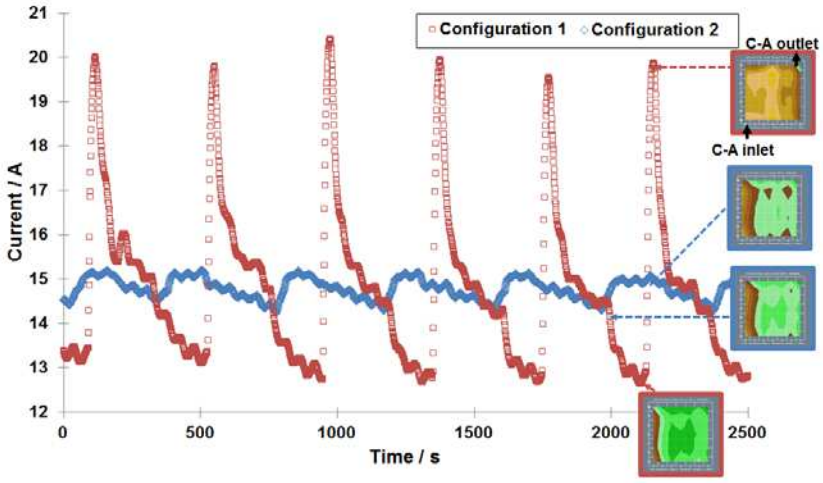

Figure 7: Channel orientation effect in a cell with a MEA perpendicular to the surface plane, configuration 1 (squares) vs. configuration 2 (diamonds) under the conditions of Table 1 in potentiostatic mode.

According to the work published by Lu et al. (37), a design corresponding to configuration 1, with channels parallel to the surface plane, enhances H_2O accumulation in the liquid state inside the channels. It has been argued above that this condition has a significant effect on prominent ignition appearance. This process can be observed in Figure 7 (squares symbols). In comparison, for configuration 2, with channel directions perpendicular to the ground plane (diamonds), the cell response exhibits a dramatically reduced ignition feature. For some of the experimental conditions applied under this configuration, ignition occurrences have been observed but always with a lower frequency than the one observed for configuration 1. Therefore, we can correlate a decrease in the liquid H_2O accumulation in the channel, as reported by Lu et al. (37), to the absence of real ignition transitions in configuration 2.

In addition to the effect of the channel orientation on the oscillatory phenomenon, it is interesting to evaluate the effect of gravity on the MEA side orientations, comparing configurations 3 and 4.

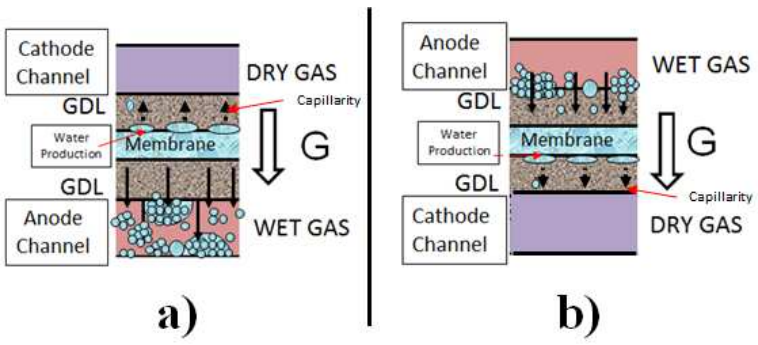

Figure 8: Cell structure schematic of (A) configuration 3 and (B) configuration 4.

In configuration 3, the well-hydrated anode is placed at the bottom of Figure 8 (a). In this manner, liquid water accumulation in the anode channel is enhanced, and we expect an increase in the ignition occurrences from the earlier observations. This configuration

also results in reduced H_2O flow from the channel to the membrane, which is associated with reduced wetting of the membrane.

In configuration 4, the anode is placed on top, enhancing the water flow from the anode channel to the membrane, as observed in Figure 8 (b).

This situation produces two different effects: on one hand, this enhancement contributes to the hydration of the membrane and, on the other hand, the enhancement reduces the liquid water accumulation in the anode channel. This effect is exacerbated by the hydrophobic properties of the GDLs, which should facilitate the water removal, thereby reducing the ignition occurrences (38).

This expectation was confirmed in the measurements presented in Figure 9, where configuration 3 exhibits prominent transitions with uniform current density distributions in the high performance level. A comparison between the low performance levels in configurations 3 and 4 reveals similar current distributions but with slightly smaller current values for configuration 3 due to the differences in the drying process associated with the orientation.

Strong transitions are observed in configurations 1 and 3, where water removal from the channel is inhibited, and no pronounced differences are observed between the two. The transitions are related to the membrane drying and wetting processes associated with the GDL (39) and channel transport properties. Therefore, previous work on the gravitational effect (40-41) has not caused effects on the internal MEA structure. However, whether the membrane thickness has an effect on the transition time remains to be evaluated.

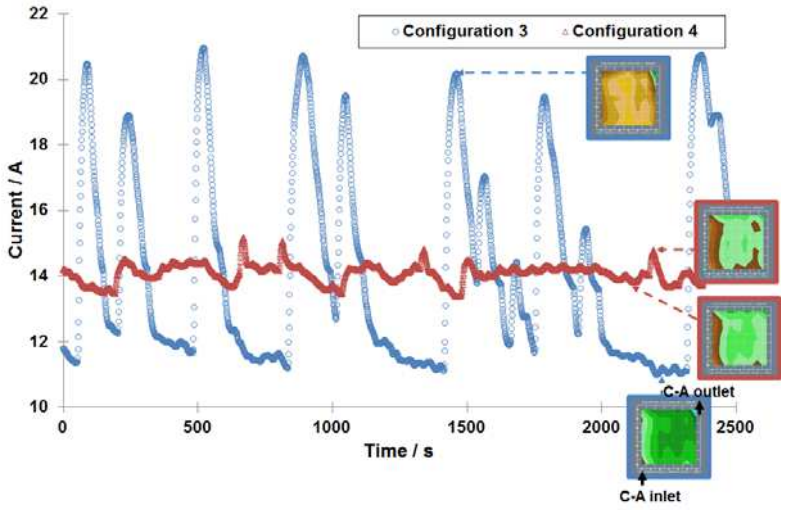

Figure 9: Cell orientation effect with MEAs parallel to the surface plane, configuration 3 (circles) vs. configuration 4 (triangles) under the conditions of Table 1 in potentiostatic mode.

Conclusions

This study describes the oscillatory response of a single polymer electrolyte fuel cell under different operation modes, namely potentiostatic versus galvanostatic modes, and the effect of cell orientation in the gravity field on the transient behavior. Oscillations appear both under galvanostatic and potentiostatic operation, and the results can be rationalized assuming a liquid water reservoir and changing water fluxes to the cathode

due to distinct water-content-dependent electro-osmotic drag rates and permeation rates (corresponding to liquid-vapor permeation). Gravitation naturally does not cause a pronounced effect on the membrane (MEA) drying or wetting process but has a significant effect on the water phase condition in the channels and on the liquid water removal process. Liquid water in the channel leads to pressure build-up and to forced convection of water through the cell. This effect has been identified as a trigger for the upward transition. Consequently, cell orientations affecting the liquid water build-up in the channel have a strong effect on the oscillatory behavior.

Consequently, this work demonstrates that the optimal configuration to work under low-humidity conditions is configuration 2, which is based on a multi-serpentine layout and favors higher flows rates than the higher relative humidities of the anode gas. This work has identified the forced convection of water as an essential process for explaining the occurrence of periodic transitions, which is essential for establishing a realistic transient model of the cell.

Acknowledgments

The authors wish to acknowledge the Deutsche Akademische Austausch Dienst (DAAD), Scholarship code number A/11/94356. The authors would also like to thank H. Sander at DLR and P. Garcia-Ibarra at the Dept. Fisica Matematica y de Fluidos (UNED) for suggestions and discussions.

References

1. R. Hanke-Rauschenbach, M. Mangold, and K. Sundmacher, Rev. Chem. Eng., 27, 23 (2011).
2. R. Hanke-Rauschenbach, M. Mangold, and K. Sundmacher, J. Electrochem. Soc., 155, B97 (2008).
3. D. Chen, W. Li, and H. Peng, J. Power Sources, 180, 461 (2008).
4. H. Sun, G. Zhang, L.J. Guo, S. Dehua, and H. Liu, J. Power Sources, 168, 400 (2007).
5. M.M. Nasef and A.A. Aly, Desalination, 287, 238 (2012).
6. R. Lin, C. Cao, J. Ma, E. Gülzow, and K. A. Friedrich, Int. J. Hydrogen Energy, 37, 3373 (2012).
7. L. A.M. Riascos, J. Power Sources, 184, 204 (2008) .
8. G.H. Guvelioglu and H.G. Stenger, J. Power Sources, 163, 882 (2007).
9. D. Hyun and J. Kim, J. Power Sources, 126, 98 (2004).
10. Y. Hiramitsu, H. Sato, H. Hosomi, Y. Aoki, T. Harada, Y. Sakiyama, Y. Nakagawa, K. Kobayashi, and M. Hori, J. Power Sources, 195, 435 (2010).
11. D. G. Sanchez, D. G. Diaz, R. Hiesgen, I. Wehl, and K. A. Friedrich, J. Electroanal. Chem., 649, 219 (2010).
12. K. Jiao and X. Li, Prog. Energ. Combust., 37, 221 (2011).
13. Q. Duan, H. Wang, and J. Benziger, J. Membrane Sci., 392– 393, 88 (2012).
14. M. Adachi, T. Navessin, Z. Xie, F.H. Li, S. Tanaka, and S. Holdcroft, J. Membrane Sci., 364, 183 (2010).
15. N.S. Mat Hassan, W.R. Wan Daud, K. Sopian, and J. Sahari, J. Power Sources, 193, 249 (2009).
16. S. Hamel and L.G. Fréchette, J. Power Sources, 196, 6242 (2011).
17. M.V. Williams, H.R. Kunz, and J.M. Fenton, J. Power Sources, 135, 122 (2004).
18. C.I. Lee and H.S. Chu, J. Power Sources, 161, 949 (2006).

19. E. Hontañon, M.J. Escudero, C. Bautista , P.L. Garcia-Ybarra, and L. Daza, J. Power Sources, 86, 363 (2000).
20. S. Dutta, S. Shimpalee, and J.W. Van Zee, J. Appl. Electrochem., 30, 135 (2000).
21. Y. Wang and C.Y. Wang, Electrochim. Acta, 51, 3924 (2006).
22. D. H. Jeon, K. N. Kim, S. M. Baek, and J. H. Nam, Int. J. Hydrogen Energ., 36, 12499 (2011).
23. T.C. Yau, M. Cimenti, X. Bi, and J. Stumper, J. Power Sources, 196, 9437 (2011).
24. Y. Lee, B. Kim, and Y. Kim, Int. J. Hydrogen Energ., 34, 1999 (2009).
25. H.K. Hsuen and K.M. Yin, Electrochim. Acta., 62, 447 (2012).
26. H. Fukumoto, H. Maeda, and K. Mitsuda, Electrochemistry, 68, 794 (2000).
27. J.R. Atkins, S.C. Savett, and S.E. Creager, J. Power Sources 128 (2004) 201-207.
28. D. G. Sanchez and P. L. Garcia-Ybarra, Int. J. Hydrogen Energ., 37, 7279 (2012).
29. J. Benziger, E. Chia, J.F. Moxley, and I.G. Kevrekidis, Chem. Eng. Sci., 60, 1743 (2005).
30. I. Nazarov and K. Promislow, Chem. Eng. Sci., 61, 3198 (2006).
31. E. Gulzow, M. Schulze, N. Wagner, T. Kaz, R. Reissner, G. Steinhilber, A. Schneider, J. ower Sources 86 (2000) 352.
32. M. Schulze, E. Gulzow, S. Schonbauer, T. Knori, and R. Reissner, J. Power Sources, 173, 19 (2007).
33. Z. Lu, S.G. Kandlikar, C. Rath, M. Grimm, W. Domigan, A.D. White, M. Hardbarger, J.P. Owejan, and T.A. Trabold, Int. J. Hydrogen Energ., 34, 3445 (2009).
34. S. Ge and C.Y. Wang, J. Electrochem. Soc., 154, B998 (2007).
35. K. Tüber, D. Pocza, and C Hebling, J. Power Sources, 124, 403 (2003).
36. J. Eller, T. Rosen, F. Marone, M. Stampanoni, A.Wokaun, and F. N. Büchi, J. Electrochem. Soc., 158, B963 (2011).
37. Z. Lu, C. Rath, G. Zhang, and S.G. Kandlikar, Int. J. Hydrogen Energ, 36, 9875 (2011).
38. S. Dusan and K. Ajay, J. Power Sources, 170, 334 (2007).
39. Z. Lu, M. M. Daino, C. Rath, and S.G. Kandlikar, Int. J. Hydrogen Energ, 35, 4233 (2010).
40. F. Y. Zhang, X. G. Yang, and C. Y. Wang, J. Electrochem. Soc., 153, A225 (2006).
41. C.E. Colosqui, M. J. Cheah, I.G. Kevrekidis, and J.B. Benzinger. J. Power Sources, 196, 10057 (2011).